

ABE-CLIP: Training-Free Attribute Binding Enhancement for Compositional Image-Text Matching

Qi Zhang¹, Yuxu Chen², Lei Deng², Lili Shen¹

¹School of Mathematics, Sichuan University

²Independent Researcher

Abstract

Contrastive Language-Image Pretraining (CLIP) has achieved remarkable performance in various multimodal tasks. However, it still struggles with compositional image-text matching, particularly in accurately associating objects with their corresponding attributes, because its inherent global representation often overlooks the fine-grained semantic for attribute binding. Existing methods often require additional training or extensive hard-negative sampling, yet they frequently yield limited generalization ability to novel compositional concepts and struggle to fundamentally address the global representation’s inherent drawbacks. In this paper, we propose ABE-CLIP, a novel training-free Attribute Binding Enhancement method designed to strengthen the attribute-object binding capability of CLIP-like models. Specifically, we first employ the Semantic Refinement Mechanism to refine the token embedding for both object and attribute phrases within the text description, thereby mitigating attribute confusion and enhancing semantic precision. Subsequently, the Local Token-Patch Local Alignment is introduced to calculate the similarity scores of the refined textual tokens to its most related patches. By intelligently aggregating the localized similarity scores, ABE-CLIP computes the final image-text similarity. Experiments on multiple datasets demonstrate that ABE-CLIP achieves significant improvements in attribute-object binding, even surpassing the methods that require extensive training.

1. Introduction

Image-text matching [23, 31] is a fundamental task in multimodal learning that aims to measure the semantic correspondence between visual content and textual descriptions. With recent advances in multimodal pre-training, contrastive learning—pioneered by CLIP [33]—has emerged as one of the dominant paradigm. CLIP [33] has demonstrated exceptional performance in multimodal tasks, such

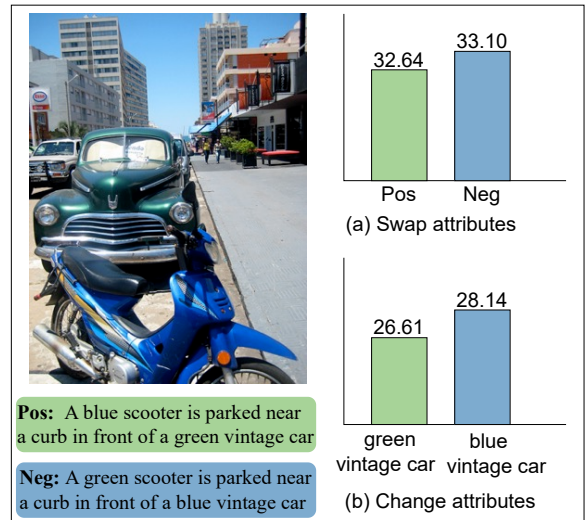


Figure 1. This illustration shows that CLIP fails to bind the attribute “green” to the corresponding object “vintage car”. (a) The positive captions and the negative captions contain identical words while the attributes are swapped; (b) The CLIP similarity between the picture and the phrases “green vintage car” and “blue vintage car”.

as image-text retrieval [28, 36, 48], image captioning [22, 26, 42] and visual question answering [11, 20, 29, 39]. Specifically, CLIP adopts a dual-tower architecture, where separate image encoder and text encoder separately extract visual and textual global feature vectors. The similarity between an image and a text is measured by the cosine similarity of their global feature vectors in a shared embedding space. This global vector representation enables high efficiency in retrieval tasks, making CLIP widely adopted in image-text retrieval scenarios.

However, the global image-text embeddings learned by CLIP often struggle with compositional semantic understanding, particularly when required to accurately bind attributes to objects in complex scenes with multiple entities.

Evidence indicates that the global representation vectors of CLIP learns disentangled, bag-of-words-style representations [44], which fundamentally limits its ability to capture finer-grained compositional information. As illustrated in Fig. 1(a), CLIP struggles to distinguish the positive caption “A blue scooter is parked near a curb in front of a green vintage car” from the negative caption “A green scooter is parked near a curb in front of a blue vintage car” when attributes are swapped. This failure reveals that relying solely on the cosine similarity between CLIP’s global image and text embedding is insufficient for fine-grained semantic understanding in compositional image–text matching.

To overcome the aforementioned limitations in compositional understanding, various methods have been proposed to enhance the fine-grained matching capability of CLIP-like models. The predominant strategy among existing approaches is to leverage hard negative examples to force CLIP-like models to discern subtle textual or visual differences [2, 13, 16, 44, 49]. Although these methods have improved compositional understanding of CLIP-like models to some extent, they still yield limited generalization to unseen compositions. In practice, such pipelines often overfit to dataset-construction artifacts and remain brittle, frequently misjudging simple relations or swapping attributes across co-occurring objects under minor perturbations. Different from hard-negative sampling, OC-CLIP [1] enhances the ability of CLIP-based architectures to learn attribute–object binding by incorporating an object-centric cross-modal binding module. However, its structured head increases architectural complexity and depends on accurate text-to-scene-graph parsing.

Alternatively, some compositional retrieval methods, like ComCLIP [15], employ a strategy that decomposes captions into multiple phrases, retrieves each phrase independently, and ultimately aggregates the phrase-level similarity scores to mitigate CLIP’s limitations in addressing attribute binding and other compositional challenges. However, determining the optimal fine-grained level for phrase decomposition remains a non-trivial challenge. If attributes and their corresponding objects are split into separate phrases, compositional retrieval still fails to bind attributes to objects effectively. When an attribute and its associated object are decomposed into a single phrase, the CLIP model may still struggle to accurately match the attribute-object pair. For instance, as demonstrated in Fig. 1(b), the similarity score between the image and the phrase “green vintage car” is lower than that between the image and the phrase “blue vintage car”, which is contradict to the ground truth. Therefore, simply decomposing captions is insufficient to effectively address the attribute binding problem.

In this work, we aim to enhance the attribute binding ability of CLIP-based models, a fundamental factor for

compositional understanding of multiple objects in complex scenes. We propose a novel plug-in and training-free framework based on CLIP-like models, named **ABE-CLIP**, which overcome the limitations of the existing text decomposition-based methods. Specifically, we propose a Local Token-Patch Alignment that computes the similarity between each text token and individual image patches, selects the patches with high similarities to each token, and thereby binds each text token to corresponding local patches. This design models the fine-grained semantic associations between textual units and image regions, while suppressing the interference from irrelevant patches, laying a solid foundation for accurate cross-modal alignment at the local level. To mitigate attribute confusion in the text modality, we incorporate a Semantic Refinement Mechanism that refines text embeddings specific to objects and attributes. This mechanism facilitates the disentanglement of object and attribute representations, yielding more discriminative vector embeddings for each text token. Besides, we put forward a Binding Difference Scores to directly assess the effectiveness of representation refinement, and its output can serve as one component of the final image-text similarity score. Lastly, we leverage above components to design an overall image–text matching score. The widely experiments on multiple benchmarks shows that the proposed method achieves state-of-the-art performance compared to existing approaches.

Our contributions can be summarized as follows:

- We propose **ABE-CLIP**, a training-free method that effectively enhances the attribute binding capability of CLIP-based models. As a plug-and-play framework, it can be seamlessly integrated into all CLIP-like models.
- ABE-CLIP integrates representation refinement and local token-patch alignment, overcoming the limitations of previous text decomposition-based approaches.
- We conduct experiments on multiple image-text matching benchmarks, and the results demonstrate that our method achieves substantial improvements in attribute binding accuracy, outperforming other existing approaches.

2. Preliminaries and Related Work

Pretrained Contrastive Vision–Language Models.

Vision–language models (VLMs) pretrained on large-scale image–text pairs have demonstrated impressive performance in multimodal domains [14, 19, 27, 33, 35]. Following CLIP [33], contrastive pretraining has become a prevalent strategy that aligns image and text representations in a shared embedding space by pulling together matched image–text pairs and pushing apart mismatched pairs in a dual-encoder setup [14, 19, 27, 34, 46, 47]. However, such global alignment objectives often struggle to capture fine-grained semantic details, which is crucial for compositional image-text understanding-particularly

in recognizing object attributes [37, 44, 52]. To address these limitations, a number of fine-grained approaches have been proposed [30, 40, 41, 53]. For example, FILIP [41] proposes a fine-grained, cross-modal late-interaction objective that aligns text tokens with image patches by max-pooling token-level similarities. GLIP [21] and RegionCLIP [53] pretrain on region-text pairs, thereby strengthening the model’s capacity for fine-grained region-text correspondence. However, these methods often require additional training and are prone to bias induced by spurious correlations in the pretraining data.

Attribute Binding. Attribute binding refers to a model’s ability to correctly associate textual attributes with the corresponding specific objects or regions within a visual scene, particularly in complex scenarios involving multiple objects and multiple attributes [12, 18, 37, 44, 52]. In recent work, fine-tuning with hard negative examples has become a proven strategy to enhance compositionality [13, 44, 50]. Among them, NegCLIP [44] synthesizes negative image-text pairs by sampling the nearest neighboring images and swapping caption words, and uses these negatives for fine-tuning. Additionally, Structure-CLIP [13] integrates scene graph knowledge (SGK) to enhance structured representations, and leverages SGK to construct hard negative captions that better match the underlying intent. Moreover, LABCLIP [17] improves attribute-object binding during cross-modal matching by applying a learned linear transformation to text embeddings, trained on hard negatives. Yet, these methods depend on hard-negative mining or enhancing structure representations, and still leave attribute-object binding implicit, leading to brittle improvements on unseen compositions.

Representation Refinement. Recent findings suggest that learned representations are decomposable and composable [3, 5, 38]. In particular, Trager et al. [38] shows that composite concepts can be approximated as a linear combination of embedding vectors associated with different factors, termed ideal words. Berasi et al. [3] proposes a Geodesically Decomposable Embeddings framework that decomposes visual representations as a geometry-aware combination of optimal directions representing primitive concepts. These observations support representation refinement along semantically meaningful directions as a reasonable refinement strategy without retraining the backbone. For example, within text-to-image generation, Magnet [54] modifies the object embeddings by pulling target attributes while pushing irrelevant ones, showing the ability to disentangle different attributes and generate anti-prior concepts. Inspired by Magnet, [25] refines object embeddings, and biased object terms are replaced with broader concepts during diffusion sampling to reduce bias. Never-

theless, leveraging representation refinement on textual embeddings for cross-modal retrieval remains under-explored.

CLIP Contrastive Language-Image Pre-training (CLIP) [33] has emerged as one of the dominant paradigms for VLM pretraining, significantly advancing image-text alignment through large-scale datasets [4, 6–8, 14, 24, 51]. It employs a dual-encoder architecture to project both modalities into a shared semantic space and utilizes a contrastive objective that pulls matched image-text pairs closer while pushing mismatched ones apart.

Specifically, given an input image I and an input text T , the visual encoder $E_V(\cdot)$ first splits I into N non-overlapping patches, then outputs a global visual [CLS] token embedding \mathbf{v}_{cls} (for whole-image representation) and N local visual patch embeddings $\{\mathbf{v}_i\}_{i=1}^N$. Meanwhile, the text encoder $E_T(\cdot)$ processes T into a sequence of up to M textual tokens, generating a global textual [EOT] token embedding \mathbf{t}_{eot} and M local textual token embeddings $\{\mathbf{t}_j\}_{j=1}^M$, where each \mathbf{t}_j corresponds to the j -th text token. CLIP models cross-modal interactions via global alignment between the entire image and its description. This approach lacks fine-grained correspondences between specific image regions and individual words or phrases. As a result, it struggles with accurate attribute-object binding, especially the phrase-region grounding.

FG-CLIP To address this limitation, FG-CLIP [40] extends CLIP with multi-granular visual-textual alignment through two key innovations. First, it introduces a regional contrastive loss to align region features with corresponding textual phrases. Second, it employs a hard negative mining strategy that rewrites descriptions to create semantically close negatives, sharpening fine-grained discrimination. This integrated approach empowers FG-CLIP’s ability to match local text tokens with corresponding image regions, thereby enabling it to discern fine-grained visual-semantic details in complex compositional scenes, significantly boosting its performance on diverse downstream tasks.

3. Proposed Method

The fundamental limitation of standard CLIP models in image-text matching ability stems from the inherent deficiency of its single global embedding [33]. Although effective for high-level semantic alignment, the obligatory aggregation of image and text information results in a coarse, “bag-of-words” representation [44], where semantic components are linearly combine. Crucially, this aggregator nature inevitably blurs fine-grained details, making precise attribute-object binding alignment extremely difficult, severely restricting the model’s compositional capability.

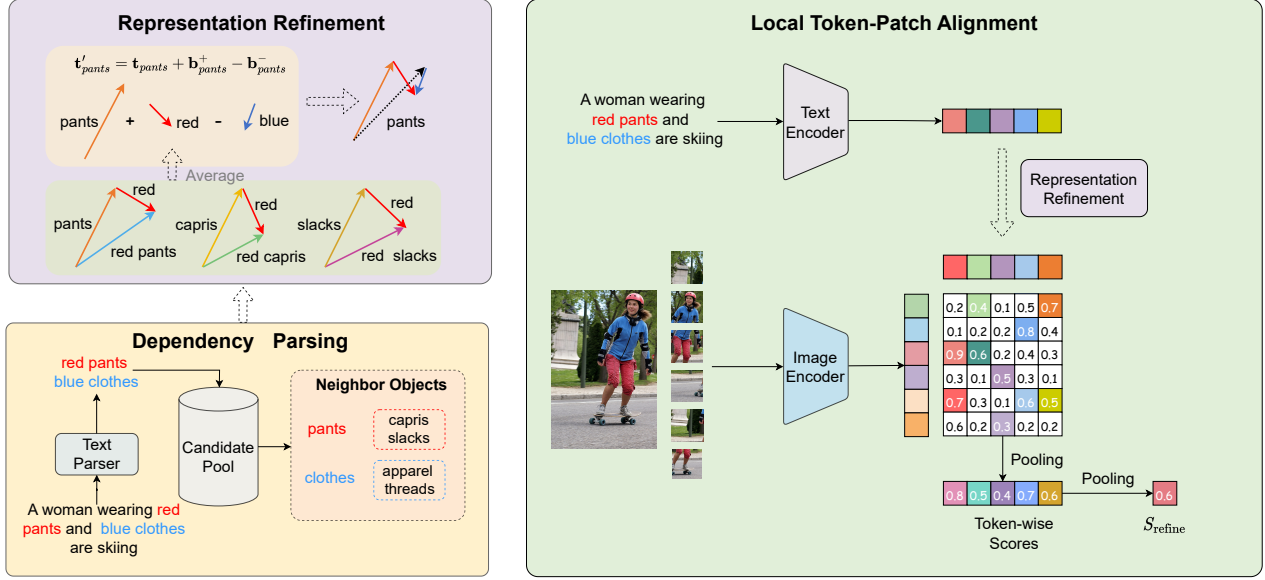


Figure 2. Overview of ABE-CLIP. Given a query caption, we first parse it to extract attribute–object phrases, then refine the attribute embedding and object embedding via Representation Refinement Mechanism. Subsequently, the Local Token-Patch Local Alignment is introduced to aggregate token–patch similarities.

We introduce **ABE-CLIP**, a training-free framework designed to enhance the ability of CLIP-based models to correctly associate attributes with their corresponding objects. The proposed method adopts a local alignment strategy, which consists of the following steps:

- Instead of relying on the similarity of coarse global vectors between images and texts, ABE-CLIP computes fine-grained token–patch similarities between the vector representations of individual text tokens and their corresponding image patches to accurately bind descriptive attributes to relevant visual objects, significantly boosting the model’s performance in compositional understanding.
- To address the limitations imposed by entangled representations of text modal, we introduce a semantic refinement mechanism. This mechanism modifies the text embeddings to facilitate attribute-object disentanglement, thereby enabling a more precise matching between words and image patches.
- Finally, by integrating global similarity, refined local matching results and the binding difference, we compute the final score to evaluate the image–text similarity.

3.1. Local Token–Patch Alignment

CLIP’s global representation paradigm is limited in capturing compositional semantics, making it difficult to accurately associate specific attributes with the correct objects [18, 45]. This is because global embeddings tend to conflate information from multiple objects and attributes within complex scenes, hindering the discrimination of spe-

cific attribute–object associations. To alleviate this problem, we take a fine-grained token–patch alignment framework to model token-wise cross-modal interactions.

Specifically, given an image–text pair (I, T) , the CLIP model encodes the image I into a sequence of visual patch embeddings $\mathbf{V} = \{\mathbf{v}_1, \dots, \mathbf{v}_N\} \in \mathbb{R}^{N \times d}$ and a visual global embedding \mathbf{v}_{cls} , and encodes the text T into a sequence of textual token embeddings $\mathbf{W} = \{\mathbf{t}_1, \dots, \mathbf{t}_M\} \in \mathbb{R}^{M \times d}$ and a textual global embedding \mathbf{t}_{eot} . The semantic correspondence between textual tokens and visual patches is characterized by their cosine similarity:

$$S_{i,j} = \frac{\mathbf{t}_i^T \mathbf{v}_j}{\|\mathbf{t}_i\|_2 \|\mathbf{v}_j\|_2}, \quad \mathbf{S} \in \mathbb{R}^{M \times N}. \quad (1)$$

For each textual token \mathbf{t}_i , we select the top- K most similar patches, forming an index set

$$\mathcal{P}_i = \arg \text{top-}K \{ S_{i,j} \}_{j=1}^N, \quad |\mathcal{P}_i| = K. \quad (2)$$

Subsequently, the token-wise score for each textual token \mathbf{t}_i is defined as the average cosine similarity over its corresponding top- K patches:

$$\phi_i = \frac{1}{|\mathcal{P}_i|} \sum_{j \in \mathcal{P}_i} S_{i,j}. \quad (3)$$

Then, the overall token–patch image–text matching score is computed by averaging the token-wise similarities

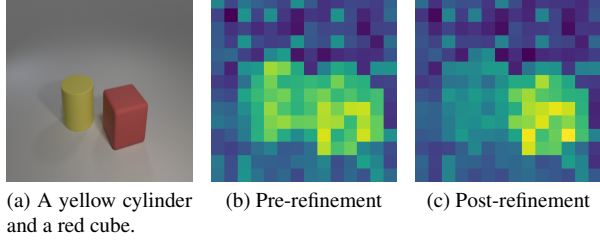


Figure 3. **Representation refinement sharpens token-patch alignment for “cube”.** (a) Input image “A yellow cylinder and a red cube.” (b,c) Similarity matrix visualizations before and after refinement between the attribute “red” and each image patch.

across all text tokens:

$$\mathcal{S}_{\text{base}}(I, T) = \frac{1}{M} \sum_{i=1}^M \phi_i. \quad (4)$$

Aggregating these local scores yields a finer-grained and more robust cross-modal alignment, thereby improving fine-grained discriminative power and interpretability in complex compositional scenes.

3.2. Semantic Refinement Mechanism

However, relying solely on the local token-patch alignment is insufficient, as it often causes attribute tokens to be attracted by patches from the wrong object. For example, in “A yellow cylinder and a red cube”, as shown in Fig. 3 (a) and (b), using unrefined contextualized token embeddings can be problematic: the attribute token *red* may be incorrectly bound to the object token *cylinder* rather than to the *cube*. Therefore, we need to modify the embeddings of the attribute and object tokens to decouple incorrect bindings and consolidate correct ones, so as to obtain more discriminative text representations. Inspired by the text-to-image generation model Magnet [54], we instantiate binding vectors to explicitly steer object embeddings toward their target attributes while repelling them from irrelevant ones.

Specifically, we parse each caption c with a natural language processing tool Stanza [32] to extract the attribute-object pairs $\mathcal{D}(c) = \{(a_m, k_m)\}_{m=1}^{M_c}$, where M_c denotes the number of extracted pairs in caption c . For each object k in $\mathcal{D}(c)$ with the text embedding \mathbf{t}_k , we denote its target attribute $A_c^+(k) = a$ and the in-sentence unrelated attributes $A_c^-(k) = \{a' : (a', k') \in \mathcal{D}(c), k' \neq k\}$ respectively. We select the P nearest neighbor objects of k in the candidate pool \mathcal{C} by cosine similarity as $\mathcal{N}(k) = \{\text{obj}_i\}_{i=1}^P$.

The positive and negative binding vectors of object k are computed as follows:

$$\mathbf{b}_k^+ = \frac{1}{P} \sum_{i=1}^P (\mathcal{F}(A_c^+(k), \text{obj}_i) - \mathcal{F}(\emptyset, \text{obj}_i)) \quad (5)$$

$$\mathbf{b}_k^- = \frac{1}{P} \sum_{i=1}^P (\mathcal{F}(A_c^-(k), \text{obj}_i) - \mathcal{F}(\emptyset, \text{obj}_i)) \quad (6)$$

where \emptyset is a blank text, and $\mathcal{F}(a, \text{obj}_i)$ is the final-layer embedding of obj_i extracted from the CLIP text encoder when encoding the phrase (a, obj_i) . Unlike Magnet, which only employs a candidate pool of 614 object nouns, we adopt the more comprehensive and empirically-grounded conceptual vocabulary provided by SPLiCE [5], containing over 12K concepts. This broader conceptual basis can further improve the robustness and generalizability of complex open-world image-text alignment.

We refine the text embedding of object k via binding vectors:

$$\mathbf{t}'_k = \mathbf{t}_k + \mathbf{b}_k^+ - \mathbf{b}_k^- \quad (7)$$

In addition, the attribute embedding \mathbf{t}'_a in the initial text embeddings is modified by:

$$\mathbf{t}'_a = \mathbf{t}_a + \mathbf{t}_k \quad (8)$$

We incorporate the modified text embeddings into the token-patch alignment of Section 3.1, yielding refined similarity scores, denoted $\mathcal{S}_{\text{refine}}(I, T)$.

3.3. Calculating Final score

To assess whether the semantic refinement mechanism in Section 3.2 guides each text token toward the correct visual evidence, we evaluate local token-patch alignment *before* and *after* refinement.

Specifically, we define the binding difference score by

$$\Delta(I, T) = \|\mathcal{S}_{\text{refine}}(I, T) - \mathcal{S}_{\text{base}}(I, T)\|, \quad (9)$$

which quantifies the absolute value of the difference between the refined local similarity score and original local similarity score.

Building upon the token-level view, we construct a local matching score that combines the token-patch similarity after semantic refinement and the binding difference score that quantifies the effectiveness of semantic refinement. Concretely, we define

$$\mathcal{S}_{\text{local}}(I, T) = \mathcal{S}_{\text{refine}}(I, T) + \Delta(I, T), \quad (10)$$

From the global view, the global similarity score is calculated as the standard CLIP calculation:

$$\mathcal{S}_{\text{global}}(I, T) = \frac{\mathbf{t}_{\text{eot}}^\top \mathbf{v}_{\text{cls}}}{\|\mathbf{t}_{\text{eot}}\|_2 \|\mathbf{v}_{\text{cls}}\|_2}, \quad (11)$$

The final image-text matching score is obtained by fusing the global and local similarities:

$$\mathcal{S}_{\text{final}}(I, T) = (1 - \omega) \mathcal{S}_{\text{local}}(I, T) + \omega \mathcal{S}_{\text{global}}(I, T), \quad (12)$$

where $\omega \in [0, 1]$ is hyperparameter to balance the contributions of the global and local alignment scores. Algorithm Algorithm 1 summarizes the proposed method.

Algorithm 1: ABE-CLIP

Input: Image I , Text T , Pretrained CLIP (E_V, E_T) , parameters K, ω

Output: Final similarity score $\mathcal{S}_{\text{final}}(I, T)$

Step 1: Compute Original Similarities

$\{\mathbf{v}_i\}_{i=1}^N, \mathbf{v}_{\text{cls}} \leftarrow E_V(I);$
 $\{\mathbf{t}_j\}_{j=1}^M, \mathbf{t}_{\text{eot}} \leftarrow E_T(T);$
Global similarity $\mathcal{S}_{\text{global}} \leftarrow \cos(\mathbf{v}_{\text{cls}}, \mathbf{t}_{\text{eot}});$
 $\mathcal{S}_{i,j} = \cos(\mathbf{t}_i, \mathbf{v}_j);$
for $i = 1$ **to** M **do**
 $\mathcal{P}_i \leftarrow \arg \max_j \text{top-}K \mathcal{S}_{i,j};$
 $\phi_i \leftarrow \frac{1}{K} \sum_{j \in \mathcal{P}_i} \mathcal{S}_{i,j};$
Original local similarity $\mathcal{S}_{\text{base}} \leftarrow \frac{1}{M} \sum_{i=1}^M \phi_i;$

Step 2: Semantic Refinement

Extract attribute-object pairs $\mathcal{D}(T) = \{(a_m, k_m)\};$

for each $(a, k) \in \mathcal{D}(T)$ **do**
 $a^+ \leftarrow a, a^- \leftarrow \{a' | (a', k') \in \mathcal{D}(T), k' \neq k\};$
 $\mathbf{b}_k^+ \leftarrow \frac{1}{P} \sum_{i=1}^P [\mathcal{F}(a^+, \text{obj}_i) - \mathcal{F}(\emptyset, \text{obj}_i)];$
 $\mathbf{b}_k^- \leftarrow \frac{1}{P} \sum_{i=1}^P [\mathcal{F}(a^-, \text{obj}_i) - \mathcal{F}(\emptyset, \text{obj}_i)];$
 $\mathbf{t}'_k \leftarrow \mathbf{t}_k + \mathbf{b}_k^+ - \mathbf{b}_k^-;$
 $\mathbf{t}'_a \leftarrow \mathbf{t}_a + \mathbf{t}_k;$

Step 3: Refined Local Similarity

Compute $\mathbf{S}' \in \mathbb{R}^{M \times N}, \mathcal{S}'_{i,j} = \cos(\mathbf{t}'_i, \mathbf{v}_j);$
for $i = 1$ **to** M **do**
 $\mathcal{P}_i^{\mathcal{R}} \leftarrow \arg \max_j \text{top-}K \mathcal{S}'_{i,j};$
 $\phi_i^{\mathcal{R}} \leftarrow \frac{1}{K} \sum_{j \in \mathcal{P}_i^{\mathcal{R}}} \mathcal{S}'_{i,j};$
Refined local similarity $\mathcal{S}_{\text{Refine}} \leftarrow \frac{1}{M} \sum_{i=1}^M \phi_i^{\mathcal{R}};$

Step 4: Calculating Final Score

$\Delta(I, T) \leftarrow \|\mathcal{S}_{\text{Refine}} - \mathcal{R}_{\text{base}}\|;$
 $\mathcal{S}_{\text{local}} \leftarrow \mathcal{S}_{\text{Refine}} + \Delta(I, T);$
 $\mathcal{S}_{\text{final}} \leftarrow (1 - \omega) \cdot \mathcal{S}_{\text{local}} + \omega \cdot \mathcal{S}_{\text{global}};$
return $\mathcal{S}_{\text{final}}$

4. Experiments

4.1. Experiment Settings

4.1.1. Datasets

We evaluate the proposed method on three benchmarks for attribution understanding: ARO-A [44], SugarCrepe(swap_att) [12] and ABC-6K [10]. Additionally, we conduct text-to-image retrieval (T2I) experiments on Flickr30K [43] and MSCOCO [23].

ARO-A. ARO-A is the attribution split of the Attribution, Relation, and Order (ARO) benchmark [44], comprising 117 unique attribute pairs with 28,748 test cases in total. Each example involves two objects (O_1, O_2) and two at-

tributes (A_1, A_2): the positive caption follows “the $A_1 O_1$ and the $A_2 O_2$,” while the negative caption swaps the attributes, yielding “the $A_2 O_1$ and the $A_1 O_2$.”

SugarCrepe. The dataset employs large language models to generate grammatically correct and semantically plausible hard negatives by replacing, swapping, or adding object, attribute, and relation. We evaluate on the Swap-Attribute subset SugarCrepe(swap_att), where captions are constructed by swapping attributes between objects.

ABC-6K (Attribute Binding Contrast Set). The positive captions in ABC-6K are collected from natural MSCOCO-2014 [23] captions that contain at least two color modifiers attached to different objects, while the negative counterparts are created by swapping the two color terms. Because ABC-6K is primarily introduced as a benchmark for text-to-image synthesis, with prompt-only annotations and no image identifiers, we mapped each prompt to its source MSCOCO image and constructed 3,213 image-text pairs.

4.1.2. Compared Methods

We compare the proposed method with two baselines and several representative prior methods in compositional image-text matching. Specifically, we adopt CLIP as the baseline model and evaluate ViT-B/16 and ViT-L/14 vision encoders [9] with CLIP’s standard 12-layer Transformer text encoder. We also use FG-CLIP as the global-matching baseline, using the official implementation of FG-CLIP and the publicly available pre-trained weights, which retain the fundamental architectural framework of CLIP’s visual and textual encoders. We employ two types of vision encoders: ViT-B/16 and ViT-L/14 [9], together with a base transformer with 63M parameters as text encoder. In addition, we compare against several representative compositional image-text matching methods, including NegCLIP, Structure-CLIP, CE-CLIP, LABCLIP, and DeGLA.

4.2. Results

4.2.1. Attribute Binding Evaluation

We evaluate compositional attribute binding of the proposed method with standard baselines and representative prior approaches on SugarCrepe(swap_att) [12], ARO-A [44] and ABC-6K [10]. We follow the evaluation protocol of prior benchmarks [12], where a prediction is correct if the similarity score for the positive caption is higher than for the negative caption. The results are displayed in Table 1. We performed a grid search over the parameter ω on the datasets and report the best setting, setting $\omega = 0.3$ in our experiments. The parameter K is default to 5. ABE-FG-CLIP_{B/16} achieves the best performance on ARO-A and

Table 1. Results(%) of our method, baselines and representative prior methods on the ARO-A, SugarCrepe(swap_att) and ABC-6K benchmarks. The best and second-best results are highlighted in **bold** and underlined, respectively.

Method	ARO-A	SugarCrepe	ABC-6K
CLIP _{B/16}	61.85	64.86	63.18
CLIP _{L/14}	61.63	62.46	62.43
FG-CLIP _{B/16}	64.69	71.02	72.27
FG-CLIP _{L/14}	64.34	69.82	71.62
NegCLIP(2023)	70.78	75.23	73.51
Structure-CLIP(2024)	80.5	80.5	-
CE-CLIP(2024)	76.4	77	75.23
LABCLIP(2025)	68.49	74.62	68.91
DeGLA(2025)	74.3	82.1	77.12
ABE-CLIP_{B/16}	67.12	64.86	66.26
ABE-CLIP_{L/14}	62.80	63.36	63.03
ABE-FG-CLIP_{B/16}	84.49	<u>81.98</u>	85.53
ABE-FG-CLIP_{L/14}	<u>83.75</u>	80.78	<u>84.94</u>

Table 2. Zero-shot performance(%) on text-to-image retrieval on Flickr30K and MSCOCO (R@K). The best performance is highlighted in **bold**.

Method	Flickr30k 1K Test			MSCOCO 5K Test		
	R@1	R@5	R@10	R@1	R@5	R@10
CLIP _{B/16}	62.24	85.60	91.92	33.03	58.38	69.09
CLIP _{L/14}	66.84	88.98	93.42	37.04	61.58	71.56
FG-CLIP _{B/16}	74.40	92.12	95.50	44.36	69.73	79.55
FG-CLIP _{L/14}	81.30	95.52	97.72	50.46	74.94	82.96
NegCLIP	65.70	89.46	93.74	41.51	68.44	78.62
LABCLIP	63.36	87.66	92.88	39.78	67.01	77.46
ABE-CLIP_{B/16}	62.54	85.84	92.06	33.34	58.73	69.28
ABE-CLIP_{L/14}	67.68	89.38	93.74	37.26	61.85	72.00
ABE-FG-CLIP_{B/16}	75.22	92.58	95.78	45.30	70.72	80.07
ABE-FG-CLIP_{L/14}	81.60	95.62	97.72	50.78	75.13	83.11

ABC-6K, and performs comparably to DeGLA on SugarCrepe(swap_att). Specifically, compared to its baseline FG-CLIP_{B/16}, it improves 19.80% on ARO-A, 10.96% on SugarCrepe(swap_att), and 13.26% on ABC-6K. Similar gains appear on FG-CLIP_{L/14} with 19.41%, 10.96% and 13.32% improvements respectively. Notably, ABE-FG-CLIP_{B/16} also substantially outperforms the methods that require extensive training, such as NegCLIP and LABCLIP. For example, it gains an improvement of 13.71% on ARO-A, 6.75% on SugarCrepe(swap_att), and 12.02% on ABC-6K compared to NegCLIP. When compared to vanilla CLIP_{B/16}, ABE-CLIP_{B/16} shows only minimal improvements, a stark contrast to the remarkable gains achieved by ABE-FG-CLIP. We hypothesize this discrepancy arises because vanilla CLIP relies primarily on global image-text alignment and lacks effective fine-grained local token-patch alignment, leading our local alignment mechanism to perform suboptimally. This hypothesis is supported by the vi-

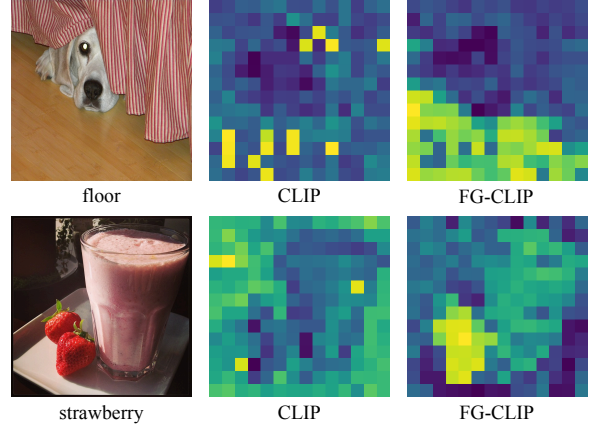


Figure 4. A comparison of similarity matrix visualizations for CLIP and FG-CLIP. We compute the similarity matrix using the words “floor” and “strawberry” with each image patch, respectively. It can be observed that CLIP fails to accurately identify the target “floor” and “strawberry”, while FG-CLIP captures some relevant visual patches.

sualizations in Fig. 4, which clearly illustrate the weakness of vanilla CLIP’s local alignment. Across backbones, enlarging the architecture from ViT-B to ViT-L does not consistently improve accuracy on compositional benchmarks. This echoes prior work showing that merely increasing model capacity does not guarantee better attribute binding.

4.2.2. Zero-Shot Cross-Modal Retrieval Evaluation

To evaluate the performance of our approach in text-to-image retrieval, we conduct experiments on the Flickr30K and MSCOCO benchmarks. We report the commonly used Recall@K (R@K) on the Flickr30K-1K test split and the MSCOCO 5K test set, as shown in Table 2. From the table, we can see that ABE-CLIP and ABE-FG-CLIP achieves slightly better performance compared to their baselines CLIP and FG-CLIP, respectively. And ABE-FG-CLIP_{L/14} achieves the best result among all compared methods. These results suggest that our method is also competitive for general image-text retrieval tasks.

4.2.3. Ablation Study

Component Analysis. We study the contribution of each component in ABE-CLIP, i.e., Local Token-Patch Alignment, Semantic Refinement Mechanism and Binding Difference Score. Experiments are conducted on ABE-FG-CLIP_{B/16}. As shown in Fig. 5, the results show that all four components are beneficial for the three benchmarks. Compared to the baseline using global representation for similarity calculation, Local Token-Patch Alignment yields substantial gains on ARO-A (+10.60%), and ABC-6K (+5.23%), with a modest change on SugarCrepe(swap_att)

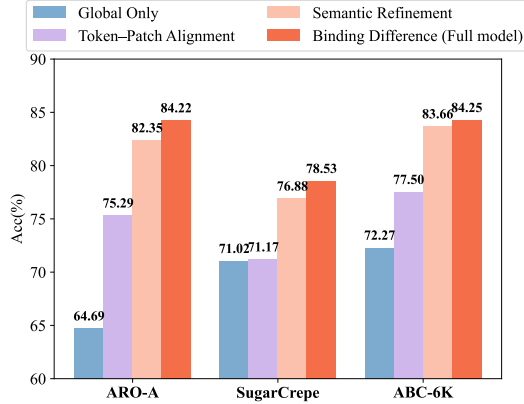


Figure 5. Results of ablation study on different components. Incorporating Local Token–Patch Alignment, the Semantic Refinement Mechanism, and Binding Difference Scores yields progressive, incremental performance gains.

(+0.15%). This indicates that global similarity alone is insufficient for capture subtle semantic difference. Introducing the Semantic Refinement Mechanism further improves performance, with an absolute gain of +7.06% on ARO-A, +5.71% on SugarCrepe(swap_att), and +6.16% on ABC-6K, respectively. This suggest that the Semantic Refinement Mechanism can effectively disentangle object-attribute relationships, enhancing the effect of local alignment of text token and image patches, and therefore improving the final results. Besides, adding the Binding Difference Score provides additional gains over the Semantic Refinement Mechanism: +1.87% on ARO-A, +1.65% on SugarCrepe(swap_att), and +0.59% on ABC-6K, respectively.

Robustness analysis on top- K Patch Pooling. For each text token, the token-wise score is computed as the the mean similarity to its top- K most similar image patches. We investigate how the number of selected patches affects performance by varying $K \in \{1, 3, 5, 8, 10\}$. As shown in Table 3, increasing K from 1 to 5 consistently improves performance: +0.93% on ARO-A, +0.15% on SugarCrepe(swap_att), and +0.81% on ABC-6K. Further increasing K to 10 results in performance saturation or slightly decline: −0.17% (ARO-A), −0.90% (SugarCrepe(swap_att)), and −0.25% (ABC-6K). This indicates that smaller K restricts the pool of spatial cues available for alignment, while larger K admits more background or distractor patches that dilute token–patch alignment. The overall effect of K on the results is not significant when K is larger than 5, which indicates that our method has strong robustness to the parameter K .

Table 3. Robustness of our method on top- K patch pooling. This table shows the results (%) on ARO-A, SugarCrepe (swap_att), and ABC-6K for different values of K from 1 to 10. The best results are highlighted in **bold**.

K	ARO-A	SugarCrepe (swap_att)	ABC-6K
1	83.56	81.83	84.72
3	84.33	81.98	85.47
5	84.49	81.98	85.53
8	84.47	81.53	85.47
10	84.32	81.08	85.28

5. Conclusion

In this paper, we present **ABE-CLIP**, a training-free, plug-and-play method aimed at enhancing attribute–object binding in compositional image–text matching. We introduce Local Token–Patch Alignment which refines the scoring by computing token-level scores via top- K patch aggregation, yielding finer-grained alignment and composition-aware similarity. To obtain finer-grained concept disentanglement, we propose Semantic Refinement Mechanism which modify the embeddings of objects and attributes.

While our work specifically addresses the attribute-binding problem in complex multi-object scenes, it does not explore other key aspects of compositional understanding, such as spatial reasoning and relational reasoning. Notably, our method holds significant potential for being extended to enhance other compositional understanding capabilities. In future work, we will explore leveraging this potential to extend our method to these capabilities, aiming to tackle a broader spectrum of visual tasks.

References

- [1] Rim Assouel, Pietro Astolfi, Florian Bordes, Michal Drozdal, and Adriana Romero-Soriano. Object-centric binding in contrastive language-image pretraining. 2025. 2
- [2] Rabiul Awal, Saba Ahmadi, Le Zhang, and Aishwarya Agrawal. Vismin: Visual minimal-change understanding. *Advances in Neural Information Processing Systems*, 37: 107795–107829, 2024. 2
- [3] Davide Berasi, Matteo Farina, Massimiliano Mancini, Elisa Ricci, and Nicola Strisciuglio. Not only text: Exploring compositionality of visual representations in vision-language models. In *CVPR*, pages 24917–24927, 2025. 3
- [4] Lucas Beyer, Andreas Steiner, André Susano Pinto, Alexander Kolesnikov, Xiao Wang, Daniel Salz, Maxim Neumann, Ibrahim Alabdulmohsin, Michael Tschannen, Emanuele Bugliarello, et al. Paligemma: A versatile 3b vlm for transfer. *arXiv preprint arXiv:2407.07726*, 2024. 3
- [5] Usha Bhalla, Alex Oesterling, Suraj Srinivas, Flavio Calmon, and Himabindu Lakkaraju. Interpreting CLIP with sparse linear concept embeddings (SPLICE). *Advances in*

- Neural Information Processing Systems*, 37:84298–84328, 2024. 3, 5
- [6] Mu Cai, Haotian Liu, Siva Karthik Mustikovela, Gregory P. Meyer, Yuning Chai, Dennis Park, and Yong Jae Lee. Vip-llava: Making large multimodal models understand arbitrary visual prompts. In *CVPR*, pages 12914–12923, 2024. 3
 - [7] Xi Chen, Xiao Wang, Soravit Changpinyo, Anthony J. Piergiovanni, Piotr Padlewski, Daniel Salz, Sebastian Goodman, Adam Grycner, Basil Mustafa, Lucas Beyer, et al. Pali: A jointly-scaled multilingual language-image model. *arXiv preprint arXiv:2209.06794*, 2022.
 - [8] Wenliang Dai, Junnan Li, Dongxu Li, Anthony Tiong, Junqi Zhao, Weisheng Wang, Boyang Li, Pascale N. Fung, and Steven Hoi. Instructblip: Towards general-purpose vision-language models with instruction tuning. In *NeurIPS*, pages 49250–49267, 2023. 3
 - [9] Alexey Dosovitskiy, Lucas Beyer, Alexander Kolesnikov, Dirk Weissenborn, Xiaohua Zhai, Thomas Unterthiner, Mostafa Dehghani, Matthias Minderer, Georg Heigold, Sylvain Gelly, et al. An image is worth 16x16 words: Transformers for image recognition at scale. In *ICLR*, 2021. 6
 - [10] Weixi Feng, Xuehai He, Tsu-Jui Fu, Varun Jampani, Arjun Akula, Pradyumna Narayana, Sugato Basu, Xin Eric Wang, and William Yang Wang. Training-free structured diffusion guidance for compositional text-to-image synthesis. *arXiv preprint arXiv:2212.05032*, 2022. 6
 - [11] Gemini Team. Gemini 1.5: Unlocking multimodal understanding across millions of tokens of context. *arXiv preprint arXiv:2403.05530*, 2024. 1
 - [12] Cheng-Yu Hsieh, Jieyu Zhang, Zixian Ma, Aniruddha Kembhavi, and Ranjay Krishna. Sugarcreeper: Fixing hackable benchmarks for vision-language compositionality. *Advances in Neural Information Processing Systems*, 36:31096–31116, 2023. 3, 6
 - [13] Yufeng Huang, Jiji Tang, Zhuo Chen, Rongsheng Zhang, Xinfeng Zhang, Weijie Chen, Zeng Zhao, Zhou Zhao, Tangjie Lv, Zhipeng Hu, et al. Structure-CLIP: Towards scene graph knowledge to enhance multi-modal structured representations. In *AAAI*, pages 2417–2425, 2024. 2, 3
 - [14] Chao Jia, Yinfei Yang, Ye Xia, Yi-Ting Chen, Zarana Parekh, Hieu Pham, Quoc Le, Yun-Hsuan Sung, Zhen Li, and Tom Duerig. Scaling up visual and vision-language representation learning with noisy text supervision. In *ICML*, pages 4904–4916. PMLR, 2021. 2, 3
 - [15] Kenan Jiang, Xuehai He, Ruize Xu, and Xin Eric Wang. ComCLIP: Training-free compositional image and text matching. *arXiv preprint arXiv:2211.13854*, 2022. 2
 - [16] Yannis Kalantidis, Mert Bulent Sariyildiz, Noe Pion, Philippe Weinzaepfel, and Diane Larlus. Hard negative mixing for contrastive learning. pages 21798–21809, 2020. 2
 - [17] Darina Koishigarina, Arnas Uselis, and Seong Joon Oh. CLIP behaves like a bag-of-words model cross-modally but not uni-modally, 2025. 3
 - [18] Martha Lewis, Nihal V Nayak, Peilin Yu, Qinan Yu, Jack Merullo, Stephen H Bach, and Ellie Pavlick. Does CLIP bind concepts? probing compositionality in large image models. *arXiv preprint arXiv:2212.10537*, 2022. 3, 4
 - [19] Junnan Li, Dongxu Li, Caiming Xiong, and Steven Hoi. Blip: Bootstrapping language-image pre-training for unified vision-language understanding and generation. In *ICML*, pages 12888–12900. PMLR, 2022. 2
 - [20] Junnan Li, Dongxu Li, Silvio Savarese, and Steven Hoi. BLIP-2: Bootstrapping language-image pre-training with frozen image encoders and large language models. In *ICML*, pages 19730–19742. PMLR, 2023. 1
 - [21] Liunian Harold Li, Pengchuan Zhang, Haotian Zhang, Jianwei Yang, Chunyuan Li, Yiwu Zhong, Lijuan Wang, Lu Yuan, Lei Zhang, Jenq-Neng Hwang, et al. Grounded language-image pre-training. In *CVPR*, pages 10965–10975, 2022. 3
 - [22] Zhang Li, Biao Yang, Qiang Liu, Zhiyin Ma, Shuo Zhang, Jingxu Yang, Yabo Sun, Yuliang Liu, and Xiang Bai. Monkey: Image resolution and text label are important things for large multi-modal models. In *CVPR*, pages 26763–26773, 2024. 1
 - [23] Tsung-Yi Lin, Michael Maire, Serge Belongie, James Hays, Pietro Perona, Deva Ramanan, Piotr Dollár, and C Lawrence Zitnick. Microsoft COCO: Common objects in context. In *ECCV*, pages 740–755, 2014. 1, 6
 - [24] Haotian Liu, Chunyuan Li, Qingyang Wu, and Yong Jae Lee. Visual instruction tuning. In *NeurIPS*, pages 34892–34916, 2023. 3
 - [25] Yueheng Luo, Tianwei Cao, Rui Wang, Ling Jin, Weidong Liu, Donghui Gao, Kongming Liang, and Zhanyu Ma. A debiasing framework for attribute binding in diffusion-based text-to-image generation. In *ICIP*, pages 1684–1689, 2025. 3
 - [26] Ron Mokady, Amir Hertz, and Amit H Bermano. CLIP-cap: CLIP prefix for image captioning. *arXiv preprint arXiv:2111.09734*, 2021. 1
 - [27] Norman Mu, Alexander Kirillov, David Wagner, and Saining Xie. Slip: Self-supervision meets language-image pre-training. In *ECCV*, pages 529–544, 2022. 2
 - [28] Jiancheng Pan, Qing Ma, and Cong Bai. A prior instruction representation framework for remote sensing image-text retrieval. In *ACM MM*, pages 611–620, 2023. 1
 - [29] Maria Pirelli, Alexandros Delitzas, Nikolas Hars, Georgios Vlassis, Sotirios Anagnostidis, Gregor Bachmann, and Thomas Hofmann. CLIP-guided vision-language pre-training for question answering in 3d scenes. In *CVPR*, pages 5607–5612, 2023. 1
 - [30] Maitreya Patel, Naga Sai Abhiram Kusumba, Sheng Cheng, Changhoon Kim, Tejas Gokhale, Chitta Baral, et al. Triplet-CLIP: Improving compositional reasoning of CLIP via synthetic vision-language negatives. 2024. 3
 - [31] Bryan A Plummer, Liwei Wang, Chris M Cervantes, Juan C Caicedo, Julia Hockenmaier, and Svetlana Lazebnik. Flickr30k entities: Collecting region-to-phrase correspondences for richer image-to-sentence models. In *ICCV*, pages 2641–2649, 2015. 1
 - [32] Peng Qi, Yuhao Zhang, Yuhui Zhang, Jason Bolton, and Christopher D Manning. Stanza: A python natural language processing toolkit for many human languages. *arXiv preprint arXiv:2003.07082*, 2020. 5

- [33] Alec Radford, Jong Wook Kim, Chris Hallacy, Aditya Ramesh, Gabriel Goh, Sandhini Agarwal, Girish Sastry, Amanda Askell, Pamela Mishkin, Jack Clark, et al. Learning transferable visual models from natural language supervision. In *ICML*, pages 8748–8763. PMLR, 2021. 1, 2, 3
- [34] Quan Sun, Yuxin Fang, Ledell Wu, Xinlong Wang, and Yue Cao. Eva-CLIP: Improved training techniques for CLIP at scale. *arXiv preprint arXiv:2303.15389*, 2023. 2
- [35] Quan Sun, Jinsheng Wang, Qiyang Yu, Yufeng Cui, Fan Zhang, Xiaosong Zhang, and Xinlong Wang. Eva-CLIP-18b: Scaling CLIP to 18 billion parameters. *arXiv preprint arXiv:2402.04252*, 2024. 2
- [36] Zeyi Sun, Ye Fang, Tong Wu, Pan Zhang, Yuhang Zang, Shu Kong, Yuanjun Xiong, Dahua Lin, and Jiaqi Wang. Alpha-CLIP: A CLIP model focusing on wherever you want. In *CVPR*, pages 13019–13029, 2024. 1
- [37] Tristan Thrush, Ryan Jiang, Max Bartolo, Amanpreet Singh, Adina Williams, Douwe Kiela, and Candace Ross. Winoground: Probing vision and language models for visio-linguistic compositionality. In *CVPR*, pages 5238–5248, 2022. 3
- [38] Matthew Trager, Pramuditha Perera, Luca Zancato, Alessandro Achille, Parminder Bhatia, and Stefano Soatto. Linear spaces of meanings: Compositional structures in vision-language models. In *ICCV*, pages 15395–15404, 2023. 3
- [39] Bin Wang, Chunyu Xie, Dawei Leng, and Yuhui Yin. Iaa: Inner-adaptor architecture empowers frozen large language model with multimodal capabilities. In *AAAI*, pages 21035–21043, 2025. 1
- [40] Chunyu Xie, Bin Wang, Fanjing Kong, Jincheng Li, Dawei Liang, Gengshen Zhang, Dawei Leng, and Yuhui Yin. Fg-CLIP: Fine-grained visual and textual alignment. *arXiv preprint arXiv:2505.05071*, 2025. 3
- [41] Lewei Yao, Runhui Huang, Lu Hou, Guansong Lu, Minzhe Niu, Hang Xu, Xiaodan Liang, Zhenguo Li, Xin Jiang, and Chunjing Xu. Filip: Fine-grained interactive language-image pre-training. *arXiv preprint arXiv:2111.07783*, 2021. 3
- [42] Yuan Yao, Tianyu Yu, Ao Zhang, Chongyi Wang, Junbo Cui, Hongji Zhu, Tianchi Cai, Haoyu Li, Weilin Zhao, Zhihui He, et al. Minicpm-V: A GPT-4V-level MLLM on your phone. *arXiv preprint arXiv:2408.01800*, 2024. 1
- [43] Peter Young, Alice Lai, Micah Hodosh, and Julia Hockenmaier. From image descriptions to visual denotations: New similarity metrics for semantic inference over event descriptions. *Transactions of the Association for Computational Linguistics*, 2:67–78, 2014. 6
- [44] Mert Yuksekgonul, Federico Bianchi, Pratyusha Kalluri, Dan Jurafsky, and James Zou. When and why vision-language models behave like bags-of-words, and what to do about it? *arXiv preprint arXiv:2210.01936*, 2022. 2, 3, 6
- [45] Yan Zeng, Xinsong Zhang, and Hang Li. Multi-grained vision-language pre-training: Aligning texts with visual concepts. *arXiv preprint arXiv:2111.08276*, 2021. 4
- [46] Xiaohua Zhai, Xiao Wang, Basil Mustafa, Andreas Steiner, Daniel Keysers, Alexander Kolesnikov, and Lucas Beyer. Lit: Zero-shot transfer with locked-image text tuning. In *CVPR*, pages 18123–18133, 2022. 2
- [47] Xiaohua Zhai, Basil Mustafa, Alexander Kolesnikov, and Lucas Beyer. Sigmoid loss for language image pre-training. In *ICCV*, pages 11975–11986, 2023. 2
- [48] Beichen Zhang, Pan Zhang, Xiaoyi Dong, Yuhang Zang, and Jiaqi Wang. Long-CLIP: Unlocking the long-text capability of CLIP. In *ECCV*, pages 310–325, 2024. 1
- [49] Jianrui Zhang, Mu Cai, Tengyang Xie, and Yong Jae Lee. Countercurate: Enhancing physical and semantic visio-linguistic compositional reasoning via counterfactual examples. *arXiv preprint arXiv:2402.13254*, 2024. 2
- [50] Le Zhang, Rabiul Awal, and Aishwarya Agrawal. Contrasting intra-modal and ranking cross-modal hard negatives to enhance visio-linguistic compositional understanding. In *CVPR*, pages 13774–13784, 2024. 3
- [51] Yuhao Zhang, Hang Jiang, Yasuhide Miura, Christopher D. Manning, and Curtis P. Langlotz. Contrastive learning of medical visual representations from paired images and text. In *MLHC*, pages 2–25. PMLR, 2022. 3
- [52] Tiancheng Zhao, Tianqi Zhang, Mingwei Zhu, Haozhan Shen, Kyusong Lee, Xiaopeng Lu, and Jianwei Yin. VI-checklist: Evaluating pre-trained vision-language models with objects, attributes and relations. *arXiv preprint arXiv:2207.00221*, 2022. 3
- [53] Yiwu Zhong, Jianwei Yang, Pengchuan Zhang, Chunyuan Li, Noel Codella, Liunian Harold Li, Luowei Zhou, Xiyang Dai, Lu Yuan, Yin Li, et al. RegionCLIP: Region-based language-image pretraining. In *CVPR*, pages 16793–16803, 2022. 3
- [54] Chenyi Zhuang, Ying Hu, and Pan Gao. Magnet: We never know how text-to-image diffusion models work, until we learn how vision-language models function. *Advances in Neural Information Processing Systems*, 37:57115–57149, 2024. 3, 5